International Journal of Nanotechnology

ISSN online: 1741-8151 - ISSN print: 1475-7435
https://www.inderscience.com/ijnt

Improved generalised fuzzy peer group with modified trilateral filter to remove mixed impulse and adaptive white Gaussian noise from colour images

Akula Suneetha, E. Srinivasa Reddy

DOI: 10.1504/IJNT.2023.10056473

Article History:

Received:	18 February 2021
Last revised:	20 April 2021
Accepted:	17 June 2021
Published online:	31 May 2023

Improved generalised fuzzy peer group with modified trilateral filter to remove mixed impulse and adaptive white Gaussian noise from colour images

Akula Suneetha*

KKR & KSR Institute of Technology and Sciences,
Department of CSE,
Guntur, 522017, Andhra Pradesh, India
Email: sunitha.akula1.cse@gmail.com
Email: sunitha_akula1@yahoo.co.in
*Corresponding author

E. Srinivasa Reddy

Department of CSE,
University College of Engineering & Technology,
Acharya Nagarjuna University,
Nagarjuna Nagar, Guntur, 522510, Andhra Pradesh, India
Email: edara_67@yahoo.com

Abstract: In image processing applications, image denoising is an emerging area that recovers the original image from noisy image, which is essential in the applications like pattern analysis. The main aim of this study is to propose an effective filtering technique with peer groups for effective image restoration processes. Existing bilateral filter has lower performance in smoothing the high curvature and high gradient regions due to nearby input signals are outliers that miss the filter window. In this research paper, a new approach is proposed that includes fuzzy-based approach and similarity function for filtering the mixed noise. In a peer group, the similarity function was adaptive to edge information and local noise level, which was utilised for detecting the similarity among pixels. In addition, a new filtering method modified trilateral filter (MTF) with improved generalised fuzzy peer group (IGFPG) is proposed to remove mixed impulse and adaptive white Gaussian noise from colour images. The modified trilateral filter includes Kikuchi algorithm and loopy belief propagation to solve the inference issues on the basis of passing local message. In this research work, the images were collected from KODAK dataset and a few real time multimedia images like Lena were also used for testing the effectiveness of the proposed methodology. The collected colour images were contaminated with adaptive white Gaussian noise (AWGN) of standard deviation $\sigma\epsilon[05,20]$ and impulse noise of probability $p\epsilon[0.05,0.20]$. The proposed MTF-IGFPG method has the advantages of consider image photometric and geometric similarities. The local structural similarity and narrow spatial window is applied for smoothing the images to effectively preserve the images. From the simulation, the proposed MTF-IGFPG approach attained better performance related to the existing approaches in light of

normalised colour difference (NCD), peak signal-to-noise ratio (PSNR), and mean absolute error (MAE). Hence, the proposed approach almost achieved PSNR of 36 dB, which shows 0.2 dB to 2 dB improvement than the existing methods.

Keywords: adaptive white Gaussian noise; belief propagation technique; impulse noise; improved generalised fuzzy peer group; Kikuchi algorithm; modified trilateral filter.

Reference to this paper should be made as follows: Suneetha, A. and Srinivasa Reddy, E. (2023) 'Improved generalised fuzzy peer group with modified trilateral filter to remove mixed impulse and adaptive white Gaussian noise from colour images', *Int. J. Nanotechnol.*, Vol. 20, Nos. 1/2/3/4, pp.129–150.

Akula Suneetha received her BTech (CSE) from Sir C R Reddy College of Engineering, Andhra University in 2005 and MTech (CSE) degree from Jawaharlal Nehru Technological University Hyderabad, Telangana, India in 2009. She is currently pursuing PhD degree in Acharya Nagarjuna University. She is currently working as Assistant professor in the Department of CSE, KKR & KSR Institute of Technology & Sciences, Guntur, Andhra Pradesh affiliated to JNTUK University. Her research area is fuzzy image processing. She is having 13 years of teaching experience.

E. Srinivasa Reddy, Professor & Dean, University College of Engineering & Technology, Acharya Nagarjuna University, A.P. He did Philosophical Doctorate in Computer Science and Engineering from Acharya Nagarjuna University, Guntur. He did Master of Technology in Computer Science and Engineering from Sir Mokhsagundam Visweswariah University, Bangalore. He also did Master of Science from Birla Institute of Technological Sciences, Pilani. He guided several research scholars of PhD. His research areas of interest are in various domains including digital image processing. He has published 5 books, 78 journals and attended 45 conferences and 24 workshops.

1 Introduction

In current scenario, eliminating noise from the digital images is an essential task due to the needs of several applications like medical images, satellite imaging, segmentation, tracking, etc. [1–5]. Generally, digital images inherit dissimilar noises from dissimilar sources such as Adaptive White Gaussian Noise (AWGN), salt and pepper noise, Gaussian noise, rician noise, impulse noise, etc. [6–8]. These noises are very hard to find accurately, so external models are required for addressing the different noise types. Denoising is the procedure of manipulating the image and eliminates the noise from the original image for developing a visually high quality digital image [9,10]. Generally, image denoising is a pre-processing technique that plays a crucial role in image analysis. The main aim of image denoising is to eliminate the noises and artefacts as best as possible from the original images without losing the image details [11,12]. Currently, dissimilar approaches are comprehensively studied for analysing and improving traditional denoising algorithms. The important aspect of solving image denoising problems is to maintain a good balance between the noise and image details [13,14].

Still, image denoising is a challenging process, especially in the applications like pattern analysis and computer vision [15,16]. Recently, several techniques are developed for image denoising, for instance, weighted hybrid regularising approach [17], hierarchical residual learning [18], deep convolutional neural network [19,20], split Bregman approach [21], low-rank Bayesian tensor factorisation [22], etc. Aforementioned techniques delivered better results in light of PSNR, mean structural similarity index matrix (MSSIM), edge-preservation index (EPI), signal-to-clutter ratio (SCR), etc.

Though, the above-mentioned methods achieved a good performance in image denoising, still the developed systems are not proven reliable for image denoising due to some imaging factors like illumination, lighting variations, etc. So, the important goal of the present research work was to develop an efficient system in order to deliver an effective noiseless image. In this paper, a new approach was proposed for estimating the noisiness of the image pixel. The proposed approach works on the basis of robust noisiness measures that were evaluated by utilising noise and edge information of pixel locality. In addition, the noisiness was used to develop a generalised fuzzy peer group with a modified trilateral filter to remove mixed AWGN and impulse noise from colour images. In modified trilateral filter, a loopy belief propagation was used to increase the smoothness of images by adjusting the similarity of weight function in IGFPG. In addition, Kikuchi algorithm was included in loopy belief propagation in order to overcome the statistical issues that arises in generalised fuzzy peer groups. Meanwhile, the Kikuchi algorithm effectively solves the inference problems by passing the local message. In the experimental section, the proposed approach was compared with other existing algorithms in light of NCD, PSNR, and MAE on KODAK dataset and a few real time multimedia images like Lena. The experimental consequences how that the proposed approach outperformed the existing systems significantly.

Some research papers on image denoising are surveyed in Section 2. The problem statement of the current research work is stated in Section 3. The mathematical explanation about the proposed methodology is represented in Section 4. The experimental outcome of the proposed methodology is given in Section 5. Finally, the conclusion of the present research work is specified in Section 6.

2 Literature survey

Dev and Verma [23] has used fuzzy peer group with modified bilateral filter for image denoising. The developed model effectively estimates the noisiness of pixel in the colour image and also it effectively preserves the image details related to the existing models. In this literature, the developed model performance was investigated on KODAK dataset, where the collected image was contaminated with Gaussian and impulse noise. Extensive experiment shows that the developed model attained better performance in image denoising by means of mean absolute error (MAE), peak signal to noise ratio (PSNR), and normalised colour difference (NCD). However, the developed model only removed the mixed noise from the colour images sufficiently, but it was not adequate for grey scale images. Further, Dev and Verma [24] developed IGFPG with modified bilateral filter, adaptive average filter, and iterative algorithm for colour image denoising. The developed model used a similarity function to detect resemblance between the pixels in a peer group. In addition, the developed model used adaptive weighted average of dissimilar sized filters. The modified bilateral filter with adaptive average filter, and

iterative algorithm effectively denoise the homogeneous regions in the images without decreasing the morphological edges. Although, bilateral filter with adaptive range and spatial parameters showed better performance in image denoising in light of PSNR, NCD, and MAE. In contrast, the computational cost of the developed model was high, so optimisation was required to achieve consistent performance.

Camarena et al. [25] has used fuzzy rank ordered differences (FROD) filter for image denoising. In this literature study, a new noise detection procedure was carried-out, which includes two major steps: filtering (median filter) and novel fuzzy context. Experimental simulation showed that the developed model delivers better results for impulse noise reduction and computationally effective. In this literature, the developed model performance was analysed using KODAK dataset in light of MAE, PSNR, and NCD. However, Wiener filter was a statistical approach, which was relatively expensive and computationally complex. Though, wiener filter requires an accurate noise model; or else, it was very difficult to apply in real time images. Florea et al. [26] has used discrete cosine transform (DCT) with sparse representation for image denoising. The developed model was numerically efficient and it automatically adjusts the thresholding value based on noise level that significantly reduces the system complexity. In this literature, the developed model performance was analysed on KODAK dataset by means of PSNR, MSE, and MSSIM. The major drawback of the developed model was it used median values to restore the noisy pixels, where in grey scale images the median values were highly corrupted.

Morillas et al. [27] has used fuzzy peer group with fuzzy average filter for image denoising. The developed method effectively supresses the both impulse and Gaussian noise and mixed Impulse-Gaussian noise. Experimental result showed that the developed filter attains a promising performance in image denoising by means of PSNR, MAE, and NCD. While performing with two stage procedure (fuzzy peer group with fuzzy average filtering), the computational complexity was bit high. Shakeri et al. [28] has used fuzzy clustering and sub histogram equalisation for image denoising. The developed model effectively enhanced the image contrast by performing three steps. Initially, histogram analysis was performed to estimate the number of clusters and then determine the image brightness level using transfer functions. At last, contrast enhancement was added for each individual cluster distinctly. In this literature study, the developed model performance was investigated on KODAK and Berkeley datasets in light of feature similarity index for image (FSIM). The developed model was used to remove the Gaussian noise by preserving important image structures. However, the developed model usually wipes small features that significantly degrades the performance.

Yang et al. [29] has developed fuzzy block-matching with Gaussian denoising algorithm. The developed algorithm attains high performance related to existing denoising algorithms in both real RAW and standard test images by means of PSNR and SSIM. The developed algorithm performance was analysed on the multimedia images (Peppers, Lena, and Baboon) and the images were contaminated with Gaussian and Poisson noise. The developed denoising algorithm has a disadvantage in the practical case of sparse matrices, because it consumes more memory and potentially more time. Ananthi et al. [30] has used fuzzy-set technique, which was tested with five different filtering methods for image denoising. The developed method achieved better denoised results related to other existing methods. The computational time of the developed method was trice less related to other denoising methods in the colour images. In this literature, the developed method performance was analysed on the multimedia images

which were contaminated with impulse noise. The developed method showed good performance in impulse noise, but it was not applicable for other noises like rician noise, salt and pepper noise, etc.

3 Problem statement

Generally, in image denoising, filtering approaches are mainly used to suppress high and low frequencies in the colour images that effectively enhances and detects the edges in input images [31–33]. Hence, filtering methodologies plays a significant role in image denoising [34,35]. Depending on the type of noises, a suitable filter is adapted for denoising the colour images [36–38]. For instance, the filtering methodologies like bilateral filter smooths the sharp changes in ridge like features or valley, gradients, blurring ramp edges or blunting. In contrast, the bilateral filter poorly smooths the high curvature and high gradient regions, because most of the nearby input signals are outliers that misses the filter window [39,40]. To avoid these issues, IGFPG with modified trilateral filter is proposed to effectively denoise the colour images, which are contaminated with AWGN and impulse noise.

Solution: By analysing dissimilar filters, trilateral filter is better to preserve the edges in high gradient region of the digital images. In addition, trilateral filter delivers good approximate scene illumination, as a sharply bounded piece-wise smooth signal with local gradient. Still, the trilateral filter degrades the image details (for example, image edge information) and it is computationally expensive. In this paper, a new approach is proposed for determining the peer group to denoise the digital images. The proposed peer group is named as IGFPG, which is evaluated by edge information and similarity function in the color images on the basis local noise level. The IGFPG is utilised for suppressing the mixed impulse and AWGN from the colour images. For filtering, modified trilateral filtering approach is proposed with adaptive edge information. In the modified trilateral filter, a loopy belief propagation is used to increase the image smoothness by adjusting the similarity of weight function in IGFPG. In addition, Kikuchi algorithm is included to overcome the statistical issues that arise in loopy belief propagation. Kikuchi algorithm effectively solves the inference issues based on passing local message.

4 Proposed methodology

In image processing, image denoising is an elementary issue that is encountered in some real time applications such as visual tracking, image restoration, registration, etc. Theoretically, it is tough to precisely recuperate an image from noise, because it is a highly under-constrained issue [41,42]. For instance, distortion due to AWGN is caused by transmitting the image data in noisy communication and by poor quality image collection. In recent decades, pixel level filtering approaches such as Gaussian filtering, patch level filtering method, and bilateral filter greatly preserves the image details, when the image is too noisy [43]. The performance of denoising drops extremely with respect to increase in noise levels.

4.1 Data collection

Initially, the original image is collected from KODAK database and also a few multimedia images like Lena are also used for experimental evaluation. The KODAK database is collected by Eastman Kodak Company that produces camera related products with its historic basis on photography. The KODAK dataset comprises of 25 uncompressed Portable Graphics Format (PNG) true colour images with the size of 768×512. The sample images of KODAK dataset are graphically denoted in Figure 1. After data collection, image denoising is carried-out utilising IGFPGwith trilateral filter.

Figure 1 (a) Flower image, (b) Parrots image and (c) Lena image (see online version for colours)

(a) (b)

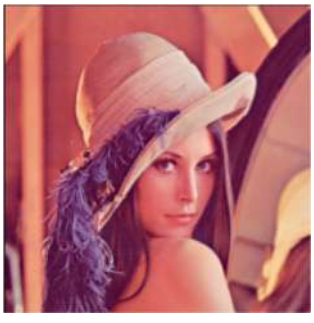

(c)

4.2 Improved generalised fuzzy peer group with modified trilateral filter

Generally, the term 'peer group' is defined as a set of pixels selected from neighbourhood pixels under consideration that effectively helps in diminishing the noise. The elements, which are closer to the actual value of centre pixel, have better filtering. There are two general aspects to obtain a peer group: (i) a similarity function is utilised to sort the neighbourhood pixels that determines the peer group with an appropriate algorithm, (ii) the undertaken algorithm should select best elements from the ordered set utilising similarity function. In this research work, an effective Gaussian membership function (GMF) is used to calculate the similarity function.

In this segment, the input colour image is denoted as $I(x)$ with the size of $m\times n$, where x is indicated as three dimensional vector. Let, the vector $x=\{p,q,k\}$, and the generic vector $I_{pq}(x)\in I(x)$ is an image pixel at x, which is expressed as $I_{pq}(x)=\{I_{pq}^{R},I_{pq}^{G},I_{pq}^{B}\}$ in RGB colour space. In this research work, S_h^k is represented as

sliding window at centred pixel $I_{pq}(x)$, h is indicated as half window size, and k is denoted as RGB colour space, where $k=1$ for red colour, $k=2$ for green colour, and $k=3$ for blue colour. The size of sliding window is evaluated using equation (1).

$$H=(2h+1)\times(2h+1) \tag{1}$$

If the size of window $h=0$, single pixel $I_{pq}(x)$ is considered, and the window size $h=1$ represents 3×3 pixel value. Similarly, $n_{pq}^{h,k}$ is specified as a neighbourhood pixel set, which is mathematically expressed in equation (2).

$$n_{pq}^{h,k}=\left\{i_p+u,q+v\forall u,v\epsilon\left[-h,h\right]\right\} \tag{2}$$

Let, $\rho(c_{pq},i_N)$ is stated as similarity function, where c_{pq} is denoted as generic centre pixel intensity of I_{pq}^{k} and $i_N\epsilon n_{p,q}^{h,k}$. The similarity function $\rho(c_{pq},i_N)$ is mathematically denoted in equation (3).

$$\rho(c_{pq},i_N)=e^{-0.5\left(\frac{c_{pq}-i_N}{\sigma_{pq}}\right)^2} \tag{3}$$

where, c_{pq} is denoted as edge function, σ_{pq} is represented as noise function, and σ_{pq} is stated as variance adaptive to each I_{pq}^{k} pixel under processing. The undertaken similarity function is more general, because of using centre intensity c_{pq} instead of centre pixel.

4.2.1 Local noise and edge information

In this research, a new fuzzy rule based approach is developed for estimating the true centre intensity by assuming noise level and edge. On the basis of central limit theorem, standard deviation of the mean distribution of sample size N is $(1/\sqrt{N})$th of standard deviation of the parent distribution. The central limit theorem is true for any sample size N, because impulse and AWGN are Gaussian distribution. If the mean is considered for N number of pixels, the standard deviation of impulse and AWGN mean is $(1/\sqrt{N})$th. Though, the mean comprises of two different noise levels for two different sample size N. Estimate the noise qualitatively in colour image by using several sample size N. Hence, the use of fuzzy logic delivers an appropriate estimation of noise.

Let, $M_{pq}^{k}(h)$ is considered as a mean of pixel intensity over sliding filter window of half window size h with centre of the filter window I_{pq}^{k}, and $d_{pq}^{k}(h)$ is represented as the gradient of $M_{pq}^{k}(h)$. The mathematical equations to calculate $M_{pq}^{k}(h)$ and $d_{pq}^{k}(h)$ are expressed in the equations (4) and (5).

$$M_{pq}^{k}(h)=\frac{1}{H}\sum_{N=1}^{H}i_N,i_N\epsilon n_{p,q}^{h,k} \tag{4}$$

$$d_{pq}^{k}(h)=M_{pq}^{k}(h)-M_{pq}^{k}(h-1),d_{pq}^{k}(0)=0 \tag{5}$$

Let, $T_{|d|}$ is denoted as threshold, and D_{pq}^{k} is stated as a set of gradients $d_{pq}^{k}(h)$, whose absolute value is greater than $T_{|d|}$ that is mathematically denoted in equation (6). Let,

consider $Cd\left(D_{pq}^{k}\right)$ as cardinality of D_{pq}^{k}, and the threshold T_n decides whether $Cd\left(D_{pq}^{k}\right)$ is low or high to forecast local noise level. The local noise and edge information is obtained by using Table 1.

$$D_{pq}^{k}=\{d_{pq}^{k}(h)|\forall h\, s.t.\left|d_{pq}^{k}(h)\right|>T_{|d|}\} \tag{6}$$

Table 1 Edge and noise data utilising $Cd\left(D_{pq}^{k}\right)$ and $M_{pq}^{k}(h)$

Case	$M_{pq}^{k}(h)$	$Cd\left(D_{pq}^{k}\right)$	*Edge*	*Noise*
1	Non-monotonic	$\geq T_n$	Yes	High
2	Monotonic	$\geq T_n$	No	High
3	Non-monotonic	$< T_n$	Yes	Low
4	Monotonic	$< T_n$	No	Low

4.2.2 Robust noisiness measure

In this segment, a new method is developed for estimating the noisiness of image pixels that depends on several filter sizes. Let, R_{pq}^{k} is the developed noisiness measure of $I_{pq}^{k}\epsilon I(x)$ that is denoted in equation (7).

$$R_{pq}^{k}=\frac{\sum_{h=0}^{4}s_{pq}^{k}(h)\left|M_{pq}^{k}(h)-I_{pq}^{k}\right|}{\sum_{h=0}^{4}s_{pq}^{k}(h)} \tag{7}$$

where, $M_{pq}^{k}(h)$ is mathematically defined in the equation (4), and s_{pq}^{k} is a weight function used to differentiate the pixels with several means. The weight function s_{pq}^{k} is adaptive to local noise and edge information that is calculated by utilising three fuzzy IF-THEN rule for dissimilar cases of noise and edge information as denoted in Table 1.

- IF (case 1 and 4) THEN $s_{pq}^{k}=f_3(h)$
- IF (case 3) THEN $s_{pq}^{k}=f_2(h)$
- IF (case 2) THEN $s_{pq}^{k}=f_1(h)$

The functions $f_1(h)$, $f_2(h)$, and $f_3(h)$ are graphically denoted in Figure 2. The higher window size has more weights, if the noise level is HIGH and NO EDGE, which is the reason to select $f_1(h)$ for case 2. In case 3, the lower window size has more weights, if the noise level is LOW and EDGE. In other two circumstances (case 1 and 4), $f_3(h)$ is highly suitable. Equations (8)–(10) shows the mathematical expression of $f_1(h)$, $f_2(h)$, and $f_3(h)$.

$$f_1(h)=\frac{1}{4}h \tag{8}$$

$$f_2(h)=\frac{-1}{4}h+1 \tag{9}$$

$$f_3(h)=\begin{cases}\dfrac{1}{2}h & \text{if } h<2\\ \dfrac{-1}{2}(h-2)+1, & \text{Otherwise}\end{cases} \tag{10}$$

Figure 2 (a) Several cases of $s_{pq}^{k}(h)$, (b) membership function for noisiness

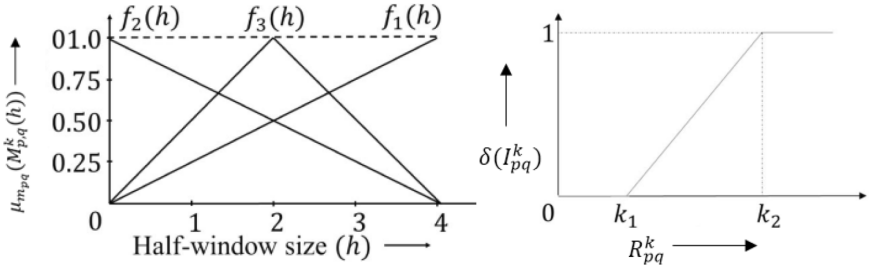

(a) (b)

In this research work, the pixel nosiness is estimated on the basis of robust noisiness measure. Let, $\delta(I_{pq}^{k})$ is represented as noisiness of the pixel I_{pq}^{k} that is mathematically stated in equation (11).

$$\delta(I_{pq}^{k})=\begin{cases}0, & R_{pq}^{k}<k_1\\ \dfrac{R_{pq}^{k}-k_1}{k_2-k_1}, & k_1<R_{pq}^{k}<k_2\\ 1, & R_{pq}^{k}>k_2\end{cases} \tag{11}$$

where, k_1 and k_2 are denoted as threshold values that decides whether a pixel is noisy or pure, and $\delta(I_{pq}^{k})$ is a function of R_{pq}^{k} as illustrated in Figure 2(b).

4.2.3 Noisiness based generalised similarity measure

Let, $\rho(c_{pq},i_N)$ is a similarity function, where c_{pq} is denoted as a generic centre of pixel intensity I_{pq}^{k}, and $i_N \epsilon n_{p,q}^{h,k}$. Similarity function $\rho(c_{pq},i_N)$ is expressed in the equations (3), (12), and (13).

$$\rho(c_{pq},i_N)=e^{-0.5}\left(\frac{c_{pq}-i_N}{\sigma_{pq}}\right)^2 \tag{3}$$

where,

$$c_{pq}=\sum_{h=0}^{4}s_{pq}^{k}(h)\times\bar{M}_{pq}^{k}(h), \tag{12}$$

$$\bar{M}_{pq}^{k}(h)=\frac{\sum_{N=1}^{H}(1-\delta(I_{pq}^{k}))\times i_N}{\sum_{N=1}^{H}(1-\delta(I_{pq}^{k}))}, \quad i_N \epsilon n_{p,q}^{h,k} \tag{13}$$

In this research study, a fuzzy set F_{pq} is included in the generalised peer group called as IGFPG. Here, $i_N \epsilon n_{pq}^{h,k}$ is related with a membership value that obtained utilising a membership function $\mu F_{pq}(i_N) : i_N \to [0,1]$. Mathematically fuzzy set is denoted in the equations (14) and (15).

$$F_{pq} = \left\{ \left(i_N, \mu F_{pq}(i_N) \right), \forall i_N \epsilon n_{pq}^{h,k} \right\}, \tag{14}$$

where,

$$\mu F_{pq}(i_N) = \rho\left(c_{pq}, i_N\right) \tag{15}$$

4.2.4 Filtering algorithm (modified trilateral filter)

In this sub-section, an effective filtering approach (modified trilateral filter) is included in IGFPG. Trilateral filter is very successful in preserving the edges. Trilateral filter is an extension of bilateral filter, and the mathematical description about the trilateral filter is illustrated below,

Bilateral filter: If $\hat{I}^h(p,q,k)$ is the estimated pixel intensity at $x = \{p,q,k\}$ in $I(x)$ with filter window size h. It is mathematically expressed in equation (16).

$$\hat{I}^h(p,q,k) = \frac{\sum_{N=1}^{H} s_N^1 s_N^2 i_N}{\sum_{N=1}^{H} s_N^1 s_N^2} \tag{16}$$

where, s_N^1 is denoted as a function of centre of intensity c_{pq}, $i_N \epsilon n_{p,q}^{h,k}$, and s_N^2 is a similar weight utilised in Gaussian filter, H is a cardinality of $n_{p,q}^{h,k}$ that is $(2h+1)\times(2h+1)$. The general equation of s_N^1 and s_N^2 are represented in the equations (17) and (18).

$$s_N^1 = \rho\left(c_{p,q}, i_N\right) \tag{17}$$

$$s_N^2 = e^{-0.5\left(\frac{\|x - x_N\|_2}{\sigma_g}\right)^2} \tag{18}$$

where, $\|.\|_2$ is denoted as L_2 norm, x is represented as central pixel position of image window, x_N is specified as pixel position i_N, σ_g is illustrated as variance of Gaussian filter that controls the value of distance based weight s_N^2.

Adaptive average filter: Let, s^h is a weight for estimated intensity using filter size h and the weighed intensity $\hat{I}(p,q,k)$ is achieved using equation (19).

$$\hat{I}(p,q,k) = \frac{\sum_{h=1}^{3} s^h \hat{I}^h(p,q,k)}{\sum_{h=1}^{3} s^h} \tag{19}$$

where, $s^h \epsilon \{0, 0.5, 1\}$, which is decided by noise and edge information as given in Table 2.

Table 2 Values of s^h for dissimilar cases

Noise and edge cases	s^1	s^2	s^3
Case 2	0	0.5	1
Case 3	1	0.5	0
Case 1 and 4	0.5	1	0.5

Trilateral filter: Trilateral filter is an extension of above-mentioned bilateral filter that abrupt the changes of range values (for instance. Jump edge, roof edge, etc.), which are easily detected using trilateral filter. The undertaken filter used directional variation of normal vectors in order to find the moderate changes in the range image. The mathematical equation of trilateral filter is denoted in equation (20).

$$\hat{I}^h(p,q,k) = \frac{\sum_{N=1}^{H} s_N^1 s_N^2 s_N^3 i_N}{\sum_{N=1}^{H} s_N^1 s_N^2 s_N^3} \tag{20}$$

where, s_N^1 is denoted as a function of centre of intensity c_{pq}, s_N^2 is a similar weight utilised in Gaussian filter, and s_N^3 is stated as a Gaussian weight function. The general equations of s_N^1, s_N^2, and s_N^3 are represented in the equations (17), (18), (21), and (22)

$$s_N^3 = e^{-0.5\left(\frac{\|I(x)-I(x)_N\|_2}{\sigma_g}\right)^2} \tag{21}$$

$$\| I(x) - I(x)_N \|_2 = \sum_{k=1}^{3} (I_k(x) - I_k(x)_N)^2 \tag{22}$$

where, $\| I(x) - I(x)_N \|$ is represented as distance between the RGB vectors at x and y, σ_g is stated as variance of Gaussian filter in spatial domain and the index represents the kth colour channel (red, blue or green).

Modified trilateral filter: In modified trilateral filter, a loopy belief propagation is included to increase the smoothing of the image by adjusting the similarity of weight function s_N^2. Let, graph P contains multiple pixels connected by multiple vertices. Then, assume label f_p to pixel p, and the energy function E_f is minimised by using equation (23). The fuzzy method estimates the approximate noise level of the images based on membership function and apply to the Modified trilateral filter.

$$E_f = \sum_{p \epsilon P} D_p(f_p) + \sum_{(p,q) \epsilon N} W(f_p, f_q) \tag{23}$$

where, $D_p(f_p)$ is denoted as a cost function, which assigns label f_p to pixel p, $W(f_p, f_q)$ is a penalty function, and N is denoted as neighbour nodes of node p. In belief propagation, the data is frequently transferred between the adjacent pixels to find the optimal label value f_p, which is mathematically denoted in equation (24).

$$m_{p \to q}^t(f_q) = \min_{f_p} \left(D_p(f_p) + W(f_p, f_q) + \sum_{s \epsilon N(p)/q} m_{s \to p}^{t-1}(f_p) \right) \tag{24}$$

In this research, Kikuchi algorithm is utilised to overcome the statistical problems that arises in belief propagation. Kikuchi algorithm effectively solves the inference issues based on passing local message. After T iterations, optimal label f_q^* is identified in order to minimise the cost functions, as given in equation (25).

$$b_q\left(f_q\right) = D_q\left(f_q\right) + \sum_{p \epsilon N(q)} m_{p \to q}^{T}\left(f_q\right) \tag{25}$$

Then, the obtained minimum cost function is include in the weight function s_N^2, and the equation (18) is updated as shown in equation (26).

$$s_N^2 = e^{-0.5\left(\frac{\|x - x_N\|_2}{\sigma_g \times m'_{p \to q}\left(f_q\right)}\right)s^2} \tag{26}$$

The cost function of equations (17), (18), and (21) are act as a membership for the cost function in equation (26). The minimum number of membership function is two and individual objective function doesn't perform denoising.

5 Simulation setup

In this section, the proposed method simulation setup such as system configuration, parameter settings, and performance measure were explained.

System configuration: For experimental simulation, MATLAB version 2018a environment was utilised with 16 GB RAM, 2 TB memory, i9 3.0 GHz processor, 2 GB GPU, and windows 10 operating system.

5.1 Parameter adjustments

There are three thresholds $T_{|d|}$, T_n, and T_I, and five parameters $\sigma_{p,q}$, σ_g, k_1, k_2, and h are used in the developed algorithm. The suitable values of three thresholds are, $T_I = 10^{-2}$, $T_n = 3$, and $T_{|d|} = 71.4$. The appropriate 'LOW' value of σ_{pq} is 45, 'HIGH' value of σ_{pq} is 110, and 'MEDIUM' value of σ_{pq} is 85. Correspondingly, σ_g is crucial to select the pixel weights on the basis of distance between central pixels. The high value of σ_g blurs the image in low noise condition. The high value of σ_g turns filter to a range filter, if the window size is low. From the experimental investigation, the most appropriate values of σ_g are identified. If $h = 1, \sigma_g = 0.8$, $h = 2, \sigma_g = 1.5$, and $h = 3, \sigma_g = 3.5$. The identification of maximum value h is vital to attain noise and edge information correctly. From the experiment analysis, the most appropriate value of h is 4.

5.2 Performance measure

In this research, the performance measures; PSNR, MAE, and NCD are utilised to analyse the relationship between input and output values of the proposed method. Generally, PSNR is defined by MAE that is mathematically denoted in equation (27).

$$MAE = 1/mn \sum_{p=0}^{m-1} \sum_{q=0}^{n-1} \| I(p,q) - k(p,q) \|^2 \tag{27}$$

where, m and n are specified as image dimension and $I(p,q)$ is represented as input image, $k(p,q)$ is denoted as reconstructed image. Another criterion used to evaluate the PSNR value is given in equation (28). Additionally, the NCD is calculated between original and denoised image by using the equation (29).

$$PSNR = 20 \log_{10} \frac{\max\left(I(p,q)\right)}{\sqrt{MSE}} \tag{28}$$

$$NCD = \frac{\sum_{p=1}^{m} \sum_{q=1}^{n} \| I_0^{LAB}(p,q,t) - I_f^{LAB}(p,q,t) \|}{\sum_{p=1}^{m} \sum_{q=1}^{n} \| I_0^{LAB}(p,q,t) \|} \tag{29}$$

where, $\|.\|$ is represented as Euclidean norm, $I_0^{LAB}(p,q,t)$ and $I_f^{LAB}(p,q,t)$ are denoted as $L^*a^*b^*$ transform of the original and denoised image. The lower NCD value has more similar (less dissimilar) images.

6 Experimental result and discussion

In this research work, three test images (flower, Lena, and parrots) were utilised to compare the performance of proposed MTF-IGFPG method with the existing methods. The proposed MTF-IGFPG method performance is assessed in light of PSNR, MAE and NCD. The images considered are contaminated with impulse noise of probability $p \epsilon [0.05, 0.20]$ and AWGN of standard deviation $\sigma \epsilon [05, 20]$.

6.1 Quantitative analysis

In this sub-section, KODAK dataset (parrot image) is used for evaluating the performance of proposed MTF-IGFPG method and existing methodsGFPG [23] and IGFPG [24] with three bilateral filters $IGFPG_{3\times3}$, $IGFPG_{5\times5}$, $IGFPG_{7\times7}$, and adaptive weighted average of dissimilar window sized filter $IGFPG_{AWW}$).In this research study, the proposed MTF-IGFPG and existing systems are validated in light of PSNR, MAE, and NCD. The image considered is contaminated with impulse noise of probability $p \epsilon [0.05, 0.20]$ and AWGN of standard deviation $\sigma \epsilon [05, 20]$. Initially, the parrot image is contaminated with mixed AWGN and impulse noise and then attempt has been carried out to reconstruct the image with high visual quality. The contaminated parrot image is shown in Figure 3(a) and then several methodologies are applied to the blurred image for restoring the contaminated image. Figures 3(b), 3(c), and 3(d) represents the restored images after applying IGFPG with bilateral filter, IGFPG with trilateral filter, and IGFPG with trilateral filter-belief propagation. At last, the restored image after applying proposed MTF-IGFPG method IGFPG with trilateral filter-belief propagation technique-Kikuchi algorithm is denoted in Figure 3(e). The part of noise image and the proposed method denoised image are shown in Figure 4(a), (b), respectively.

Figure 3 Parrot: (a) input image with $\sigma = 20,$ and $p = 0.2$, (b) bilateral filter applied image, (c) trilateral filter applied image, (d) trilateral filter with belief propagation applied image and (e) proposed method image (see online version for colours)

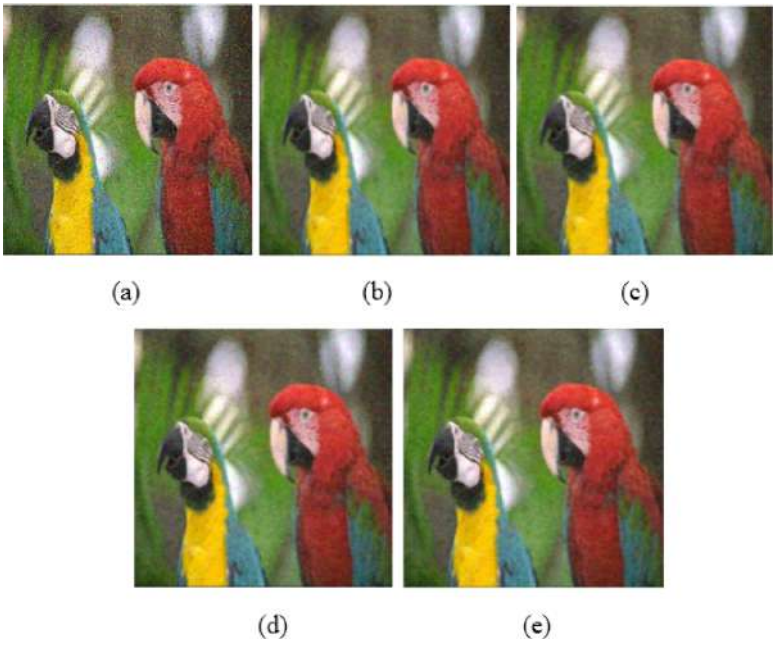

Figure 4 Parrot: (a) input image and (b) proposed method image (see online version for colours)

The sample parrot image was applied for the proposed method for denoising, as shown in Figure 4.

In Table 3, the proposed MTF-IGFPG method performance is compared with dissimilar existing methods in light of PSNR, MAE, and NCD. Meanwhile, the proposed MTF-IGFPG method performance is evaluated with different window sizes: 3×3, 5×5, 7×7, and $N\times N$. By investigating Table 3, the proposed MTF-IGFPG method delivered better performance in all three circumstances ($p = 0.05$, $\sigma = 5$), ($p = 0.1$, $\sigma = 10$), and ($p = 0.2$, $\sigma = 20$) compared to the existing approaches. In case ($p = 0.05$, $\sigma = 5$), the proposed MTF-IGFPG approach delivered maximum PSNR of 36.11dB, MAE of 2.42, and NCD of 1.98×10^{-2}. The p and σ are varied to analysis the performance of the proposed method due to its impact on the denoising. The value of p and σ are selected based on round off value.

Table 3 Performance comparison on parrot image

Noise level	*p=0.05, Sigma=5*			*p=0.1, Sigma=10*			*p=0.2, sigma=20*		
Performance metric	*PSNR (dB)*	*MAE*	*NCD* $\times 10^{-2}$	*PSNR (dB)*	*MAE*	*NCD* $\times 10^{-2}$	*PSNR (dB)*	*MAE*	*NCD* $\times 10^{-2}$
$GFPG_{3\times3}$ [23]	33.39	3.06	2.87	30.23	4.49	4.87	26.73	7.95	9.34
$GFPG_{5\times5}$ [23]	31.59	3.39	2.53	30.09	4.04	3.56	28.27	6.05	6.37
$GFPG_{7\times7}$ [23]	29.84	3.72	2.6	29.51	4.13	3.29	28.25	5.64	5.48
$GFPG_{AWW}$ [23]	31.68	3.13	2.48	30.53	3.93	3.68	28.22	6.23	6.77
$IGFPG_{3\times3}$ [24]	35.58	2.62	2.66	32.89	4.05	4.67	28.19	7.43	9.18
$IGFPG_{5\times5}$ [24]	33.25	2.94	2.29	32.61	3.55	3.32	30.16	5.48	6.12
$IGFPG_{7\times7}$ [24]	31.05	3.54	2.48	31.02	3.76	2.99	30.22	4.81	4.73
$IGFPG_{AWW}$ [24]	33.67	2.87	2.47	33.14	3.43	3.89	29.27	6.36	7.47
$IGFPG_{Bilateral}$	33.25	3.10	2.43	31.75	4.29	3.30	28.78	6.86	5.16
$IGFPG_{Trilateral}$	34.14	2.88	2.26	32.23	4.19	3.22	28.80	6.97	5.24
$IGFPG_{Trilateral-Belief}$	34.78	2.77	2.19	32.77	4.04	3.14	29.17	6.75	5.15
$Proposed_{3\times3}$	**36.11**	**2.42**	**1.98**	**33.68**	**3.37**	2.90	29.16	6.80	5.20
$Proposed_{5\times5}$	33.46	2.71	2.16	32.45	3.57	**2.78**	**30.27**	**4.52**	4.24
$Proposed_{7\times7}$	32.57	2.85	2.25	31.77	3.69	2.85	29.88	5.54	**4.23**
$Proposed_{N\times N}$	34.09	2.64	2.09	32.85	3.57	**2.78**	30.14	5.71	4.36

In Figure 5 and Table 4, the performance investigation is carried-out on flower image. The contaminated flower image is shown in Figure 4(a). Figures 4(b), 4(c), and 4(d) represents the restored images after applying IGFPG with bilateral filter, IGFPG with trilateral filter, and IGFPG with trilateral filter-belief propagation. Figure 4(e) represents the restored image after applying proposed MTF-IGFPGmethod with trilateral filter-belief propagation technique-Kikuchi algorithm). By examining Table 4, the proposed MTF-IGFPG method delivered better performance in all three cases ($p = 0.05$, $\sigma = 5$), ($p = 0.1$, $\sigma = 10$), and ($p = 0.2$, $\sigma = 20$) related to the exiting approaches with maximum PSNR of 34.53 dB, MAE of 2.85, and NCD of 2.32×10^{-2}. The proposed methodology attained better performance, because it considered both image photometric and geometric similarities, simultaneously. The result shows that proposed method preserve the quality of images and effectively removes mixed impulse and Adaptive White Gaussian Noise from colour images. The result shows that proposed method has the higher performance in denoising in various p and σ value. The analysis shows that the proposed method has decreases in the quality of images and has more error when the size of the window is increases. The proposed method has degrade in performance and increases the error in $p = 0.2$ and $\sigma = 20$. Also, the proposed MTF-IGFPG method

considered local structural similarity for smoothing the images with narrow spatial window, when preserving the images. The fuzzy generates the rules for the estimation of approximate noise based on the membership function and this is applied to trilateral filter for the denoising. The extracted local structural information is used to find the image inhomogeneity. From the experimental analysis, the proposed approach delivers better noise reduction than the bilateral filter, trilateral filter, and trilateral with belief technique.

In Figure 6 and Table 5, the performance analysis is accomplished on Lena image. From the experimental investigation, the proposed MTF-IGFPG method effectively diminishes the effect of noise in centre of intensity, since the proposed MTF-IGFPG method significantly outperforms IGFPG, and GFPG. By examining Table 5, the proposed method delivered better performance related to the exiting approaches with maximum PSNR of 36.72 dB, MAE of 2.10, and NCD of 1.93×10^{-2}. In addition, the time complexity of the proposed MTF-IGFPG method is $\theta(2t)$. In this research study, the major calculations are done twice and the algorithms are iterated t times, which is the reason to attain high visual quality noisiness image. In addition, memory complexity is calculated by $\theta(m\times n\times \max(2h+1)^2$ for $m\times n$ size image. The part of Lena noise image and proposed method denoised image are shown in Figure 7(a), (b), respectively.

Figure 5 Flower: (a) input image with $\sigma = 30,$ and $p = 0.3$, (b) bilateral filter applied image, (c) trilateral filter applied image, (d) trilateral filter with belief propagation applied image and (e) proposed method image (see online version for colours)

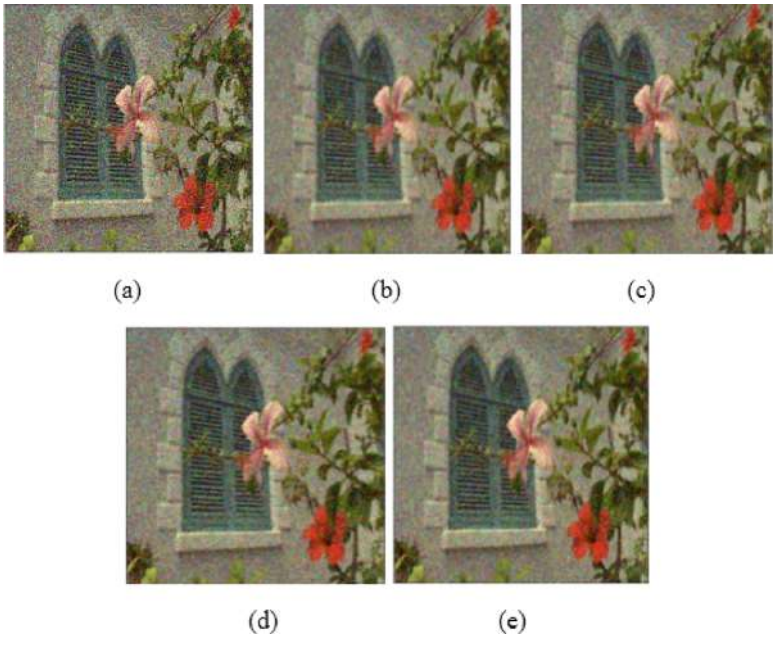

Table 4 Performance comparison on flower image

Noise level	*p = 0.05, Sigma = 5*			*p = 0.1, Sigma = 10*			*p = 0.2, sigma = 20*		
Performance metric	*PSNR (dB)*	*MAE*	*NCD*$\times 10^{-2}$	*PSNR (dB)*	*MAE*	*NCD*$\times 10^{-2}$	*PSNR (dB)*	*MAE*	*NCD*$\times 10^{-2}$
$GFPG_{3\times3}$ [23]	32.69	3.47	3.31	30.32	5.02	5.24	26.21	8.42	9.6
$GFPG_{5\times5}$ [23]	30.08	4.7	3.39	29.52	5.3	4.37	27.13	7.16	7.06
$GFPG_{7\times7}$ [23]	27.24	5.7	3.82	27.13	6.09	4.49	26.58	7.41	6.58
$GFPG_{AWW}$ [23]	30.27	4.14	3.22	29.18	4.96	4.42	27.21	7.19	7.45
$IGFPG_{3\times3}$ [24]	34.16	3.11	3.18	31.94	4.48	5.03	27.77	7.80	9.53
$IGFPG_{5\times5}$ [24]	30.04	4.16	4.02	30.61	4.65	4.12	29.02	6.32	6.74
$IGFPG_{7\times7}$ [24]	28.04	5.87	4.02	28.19	5.90	4.42	28.06	6.53	5.87
$IGFPG_{AWW}$ [24]	31.29	4.06	3.31	30.76	4.77	4.54	29.21	7.01	5.31
$IGFPG_{Bilateral}$	31.84	3.84	2.76	30.77	4.89	3.63	28.33	7.26	5.50
$IGFPG_{Trilateral}$	32.86	3.48	2.55	31.43	4.66	3.51	28.46	7.27	5.56
$IGFPG_{Trilateral-Belief}$	33.29	3.37	2.48	31.81	4.52	3.45	28.71	7.11	5.50
$Proposed_{3\times3}$	**34.53**	**2.85**	**2.32**	**32.58**	**4.12**	3.30	28.53	7.26	5.70
$Proposed_{5\times5}$	32.29	3.47	2.48	31.47	4.29	3.16	29.34	**6.21**	**4.67**
$Proposed_{7\times7}$	31.70	3.73	2.63	31.00	4.50	3.26	29.15	6.30	**4.67**
$Proposed_{N\times N}$	32.84	3.33	2.40	31.83	4.22	**3.13**	**29.36**	6.33	4.79

Figure 6 Lena: (a) input image with $\sigma = 5,$ and $p = 0.05$, (b) bilateral filter applied image, (c) trilateral filter applied image, (d) trilateral filter with belief propagation applied image and (e) proposed method image (see online version for colours)

Figure 7 Lena: (a) input image and (b) proposed method image (see online version for colours)

(a) (b)

Table 5 Performance comparison on Lena image

Noise level	*p = 0.05, Sigma = 5*			*p = 0.1, Sigma = 10*			*p = 0.2, sigma = 20*		
Performance metric	*PSNR (dB)*	*MAE*	*NCD*$\times 10^{-2}$	*PSNR (dB)*	*MAE*	*NCD*$\times 10^{-2}$	*PSNR (dB)*	*MAE*	*NCD*$\times 10^{-2}$
$GFPG_{3\times3}$ [23]	34.51	2.98	2.54	31.61	4.4	4.28	27.16	7.87	8.21
$GFPG_{5\times5}$ [23]	31.89	3.69	2.53	31.15	4.33	3.4	28.82	6.28	5.82
$GFPG_{7\times7}$ [23]	30.38	4.41	2.85	29.94	4.8	3.42	28.47	6.21	5.3
$GFPG_{AWW}$ [23]	33.13	2.28	2.39	31.82	4.11	3.44	28.75	6.39	6.16
$IGFPG_{3\times3}$ [24]	36.16	2.62	2.36	33.25	4.06	4.13	28.35	7.46	8.12
$IGFPG_{5\times5}$ [24]	33.09	3.27	2.30	32.56	3.85	3.16	30.27	5.69	5.56
$IGFPG_{7\times7}$ [24]	30.11	4.46	2.86	30.23	4.59	3.24	29.80	5.42	4.62
$IGFPG_{AWW}$ [24]	33.46	3.18	2.41	32.59	4.02	3.57	29.43	6.48	6.63
$IGFPG_{Bilateral}$	34.26	3.27	2.40	32.45	4.35	3.39	29.11	6.84	5.42
$IGFPG_{Trilateral}$	35.16	2.97	2.23	32.89	4.19	3.32	29.09	6.91	5.52
$IGFPG_{Trilateral-Belief}$	35.58	2.90	2.16	33.34	4.07	3.19	29.43	6.71	5.36
$Proposed_{3\times3}$	**36.72**	**2.10**	**1.93**	**34.08**	3.79	2.97	29.29	6.86	5.51
$Proposed_{5\times5}$	34.64	3.05	2.15	33.43	3.80	**2.84**	**30.66**	**5.36**	4.42
$Proposed_{7\times7}$	34.11	3.17	2.23	33.06	3.89	2.89	30.58	5.65	**4.39**
$Proposed_{N\times N}$	35.14	2.93	2.09	33.69	**3.77**	**2.84**	30.53	5.81	4.58

The sample medical images were applied for the proposed method for the denoising, as shown in Figure 7. The input images, bilateral filter image, trilateral filter, trilateral filter with belief propagation and proposed method is shown in Figure 8, respectively.

Figure 8 Medical image: (a) input image, (b) bilateral filter applied image, (c) trilateral filter applied image, (d) trilateral filter with belief propagation applied image and (e) proposed method image

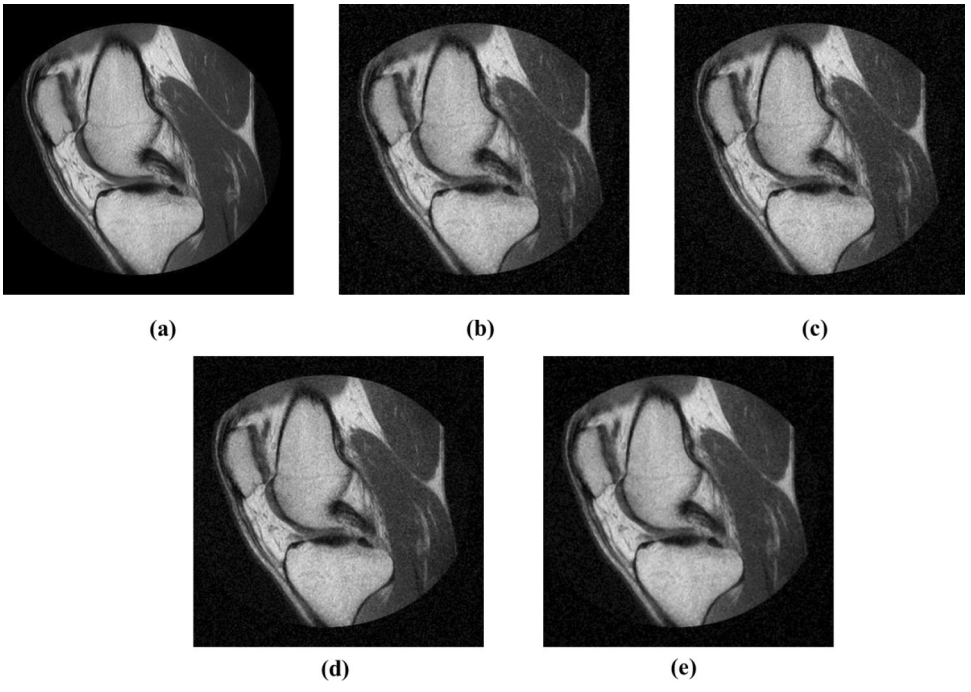

7 Conclusion

In this paper, a new method is proposed to determine peer group for denoising the colour images. The proposed peer group is named as IGFPG that is determined on the basis of edge information and local noise level in the images. The proposed peer group is utilised for suppressing the mixed AWGN and impulse noise from the colour images. For filtering, modified trilateral filter is proposed with the combination of belief propagation technique and Kikuchi algorithm. In this research study, the proposed MTF-IGFPG method is tested on KODAK dataset and a few real time multimedia images like Lena. The collected images are contaminated with impulse noise of probability $p\epsilon[0.05,0.20]$ and AWGN of standard deviation $\sigma\epsilon[05,20]$.Compared to the existing methods, the proposed MTF-IGFPG method achieved a superior performance in light of PSNR, MAE and NCD. The proposed MTF-IGFPG method effectively removes the mixed impulse and AWGN from the colour images and also preserves the quality of the images. The proposed method almost achieved PSNR of 36 dB, which shows 0.2 to 2 dB improvement than the existing methodologies. The proposed MTF-IGFPG method can be extended to the real-time applications of CCTV, Image sensor and Medical images. In future work, a new filtering approach is developed with IGFPG to further enhance efficacy of the proposed method performance for colour image denoising.

Compliance with Ethical Standards

Funding

We haven't received any funding from any sources.

Conflict of interest

The authors declare that they have no conflict of interest.

Ethical approval

This paper does not contain any studies with human participants or animals performed by any of the authors.

References

1 Asghar, M.Z., Subhan, F., Ahmad, H., Khan, W.Z., Hakak, S., Gadekallu, T.R. and Alazab, M. (2021) 'Senti□eSystem: a sentiment□based eSystem□using hybridized fuzzy and deep neural network for measuring customer satisfaction', *Software: Practice and Experience*, Vol. 51, No. 3, pp.571–594.

2 Bhattacharya, S., Maddikunta, P.K.R., Pham, Q.V., Gadekallu, T.R., Chowdhary, C.L., Alazab, M. and Piran, M.J. (2021) 'Deep learning and medical image processing for coronavirus (COVID-19) pandemic: a survey', *Sustain. Cities Soc.*, Vol. 65, p.102589.

3 Gadekallu, T.R., Rajput, D.S., Reddy, M.P.K., Lakshmanna, K., Bhattacharya, S., Singh, S., Jolfaei, A. and Alazab, M. (2020) 'A novel PCA–whale optimization-based deep neural network model for classification of tomato plant diseases using GPU', *J. Real-Time Image Process.*, pp.1–14.

4 Huang, T., Dong, W., Xie, X., Shi, G. and Bai, X. (2017) 'Mixed noise removal via Laplacian scale mixture modeling and nonlocal low-rank approximation', *IEEE Trans. Image Process.*, Vol. 26, No. 7, pp.3171–3186.

5 Yao, S., Chang, Y., Qin, X., Zhang, Y. and Zhang, T. (2018) 'Principal component dictionary-based patch grouping for image denoising', *J. Vis. Commun. Image Represent.*, Vol. 50, pp.111–122.

6 Routray, S., Ray, A.K., Mishra, C. and Palai, G. (2018) 'Efficient hybrid image denoising scheme based on SVM classification', *Optik*, Vol. 157, pp.503–511.

7 Huang, H.M. and Lin, C. (2019) 'A kernel-based image denoising method for improving parametric image generation', *Med. Image Anal.*, Vol. 55, pp.41–48.

8 Chinmay, C. (2017) 'Chronic wound image analysis by particle swarm optimization technique for tele-wound network', Springer, *Int. J. Wireless Pers. Commun.*, Vol. 96, No. 3, pp.3655–3671, ISSN: 0929-6212, 10.1007/s11277-017-4281-5.

9 Deng, L., Zhu, H., Yang, Z. and Li, Y. (2019) 'Hessian matrix-based fourth-order anisotropic diffusion filter for image denoising', *Opt. Laser Technol.*, Vol. 110, pp.184–190.

10 Chinmay, C. and Gupta, B. (2016) 'Adaptive filtering technique for chronic wound image analysis under tele-wound network', *J. Commun. Navig. Sens. Serv.*, Vol. 1, pp.57–76, 10.13052/jconasense2246-2120.2016.005.

11 He, N., Wang, J.B., Zhang, L.L. and Lu, K. (2015) 'An improved fractional-order differentiation model for image denoising', *Signal Process.*, Vol. 112, pp.180–188.

12 Shen, Y., Han, B. and Braverman, E. (2016) 'Adaptive frame-based color image denoising', *Appl. Comput. Harmon. Anal.*, Vol. 41, No. 1, pp.54–74.

13 Roy, A., Manam, L. and Laskar, R.H. (2018) 'Region adaptive fuzzy filter: an approach for removal of random-valued impulse noise', *IEEE Trans. Ind. Electron.*, Vol. 65, No. 9, pp.7268–7278.

14 Guo, S., Xiang, T. and Li, X. (2017) 'Image quality assessment based on multiscale fuzzy gradient similarity deviation', *Soft Comput.*, Vol. 21, No. 5, pp.1145–1155.

15 Zhang, Y., Xu, S., Chen, K., Liu, Z. and Chen, C.P. (2016) 'Fuzzy density weight-based support vector regression for image denoising', *Inf. Sci.*, Vol. 339, pp.175–188.

16 Chinmay, C., Gupta, B. and Ghosh, S.K. (2016) 'Tele-wound technology network for assessment of chronic wounds', *Int. J. Telemed. Clin. Practices*, Vol. 1, No. 4, pp.345–359, 10.13052/jconasense2246-2120.2016.005.

17 Islam, M.R., Xu, C., Raza, R.A. and Han, Y. (2019) 'An effective weighted hybrid regularizing approach for image noise reduction', *Circuits Syst. Signal Process.*, Vol. 38, No. 1, pp.218–241.

18 Shi, W., Jiang, F., Zhang, S., Wang, R., Zhao, D. and Zhou, H. (2019) 'Hierarchical residual learning for image denoising', *Signal Process. Image Commun.*, Vol. 76, pp.243–251.

19 Shahdoosti, H.R. and Rahemi, Z. (2019) 'Edge-preserving image denoising using a deep convolutional neural network', *Signal Process.*, Vol. 159, pp.20–32.

20 Gai, S. and Bao, Z. (2019) 'New image denoising algorithm via improved deep convolutional neural network with perceptive loss', *Expert Syst. Appl.*, Vol. 30, No. 138, p.112815, https://doi.org/10.1016/j.eswa.2019.07.032

21 Kim, J.H., Akram, F. and Choi, K.N. (2017) 'Image denoising feedback framework using split Bregman approach', *Expert Syst. Appl.*, Vol. 87, pp.252–266.

22 Wei, K. and Fu, Y. (2019) 'Low-rank Bayesian tensor factorization for hyperspectral image denoising', *Neurocomputing*, Vol. 331, pp.412–423.

23 Dev, R. and Verma, N.K. (2018) 'Generalized fuzzy peer group for removal of mixed noise from color image', *IEEE Signal Process Lett.*, Vol. 25, No. 9, pp.1330–1334.

24 Dev, R. and Verma, N.K. (2019) 'Robust noisiness measure based improved generalized fuzzy peer group for removal of mixed noise from color image', *IEEE Signal Process Lett.*, Vol. 26, No. 2, pp.267–271.

25 Camarena, J.G., Gregori, V., Morillas, S. and Sapena, A. (2010) 'Two-step fuzzy logic-based method for impulse noise detection in color images', *Pattern Recognit. Lett.*, Vol. 31, No. 13, pp.1842–1849.

26 Florea, C., Gordan, M., Vlaicu, A. and Orghidan, R. (2014) 'Computationally efficient formulation of sparse color image recovery in the JPEG compressed domain', *J. Math. Imaging Vis.*, Vol. 49, No. 1, pp.173–190.

27 Morillas, S., Gregori, V. and Hervás, A. (2009) 'Fuzzy peer groups for reducing mixed Gaussian-impulse noise from color images', *IEEE Trans. Image Process.*, Vol. 18, No. 7, pp.1452–1466.

28 Shakeri, M., Dezfoulian, M.H., Khotanlou, H., Barati, and Masoumi, Y. (2017) 'Image contrast enhancement using fuzzy clustering with adaptive cluster parameter and sub-histogram equalization', *Digital Signal Process.*, Vol. 62, pp.224–237.

29 Yang, C.C., Guo, S.M. and Tsai, J.S.H. (2017) 'Evolutionary fuzzy block-matching-based camera raw image denoising', *IEEE Trans. Cybern.*, Vol. 47, No. 9, pp.2862–2871.

30 Ananthi, V.P., Balasubramaniam, P. and Raveendran, P. (2017) 'Impulse noise detection technique based on fuzzy set', *IET Signal Process.*, Vol. 12, No. 1, pp.12–21.

31 Zhang, X., Feng, Wang, W., Zhang, S. and Dong, Q. (2013) 'Gradient-based Wiener filter for image denoising', *Comput. Electr. Eng.*, Vol. 39, No. 3, pp.934–944.

32 Nadernejad, E. and Nikpour, M. (2012) 'Image denoising using new pixon representation based on fuzzy filtering and partial differential equations', *Digital Signal Process.*, Vol. 22, No. 6, pp.913–922.

33 Wang, G., Liu, Y. and Zhao, T. (2014) 'A quaternion-based switching filter for colour image denoising', *Signal Process.*, Vol. 102, pp.216–225.

34 Singh, V., Dev, R., Dhar, N.K., Agrawal, P. and Verma, N.K. (2018) 'Adaptive type-2 fuzzy approach for filtering salt and pepper noise in grayscale images', *IEEE Trans. Fuzzy Syst.*, Vol. 26, No. 5, pp.3170–3176.

35 Chinmay, C., Gupta, B., Ghosh, S.K., Das, D. and Chakraborty, C. (2016) 'Telemedicine supported chronic wound tissue prediction using different classification approach', *J. Med. Syst.*, Vol. 40, No. 3, pp.1–12, 10.1007/s10916-015-0424-y.

36 Roy, A. and Laskar, R.H. (2016) 'Multiclass SVM based adaptive filter for removal of high density impulse noise from color images', *Appl. Soft Comput.*, Vol. 46, pp.816–826.

37 Roy, A. and Laskar, R.H. (2017) 'Non-casual linear prediction based adaptive filter for removal of high density impulse noise from color images', *AEU-Int. J. Electron. Commun.*, Vol. 72, pp.114–124.

38 Chinmay, C., Gupta, B. and Ghosh, S.K. (2016) 'Chronic wound characterization using Bayesian classifier under telemedicine framework, *Int. J. E-Health Med. Commun.*, Vol. 7, No. 1, pp.78–96, 10.4018/IJEHMC.2016010105.

39 Ngo, T.D., Bui, T.T., Pham, T.M., Thai, H.T., Nguyen, G.L. and Nguyen, T.N. (2021) 'Image deconvolution for optical small satellite with deep learning and real-time GPU acceleration', *J. Real-Time Image Process.*, Vol. 18, No. 5, pp.1697–710.

40 Vu, D.L., Nguyen, T.K., Nguyen, T.V., Nguyen, T.N., Massacci, F. and Phung, P.H. (2020) 'HIT4Mal: hybrid image transformation for malware classification', *Trans. Emerg. Telecommuni. Technol.*, Vol. 31, No. 11, p.e3789.

41 Zhang, X. and Ye, W. (2017) 'An adaptive fourth-order partial differential equation for image denoising', *Comput. Math. Appl.*, Vol. 74, No. 10, pp.2529–2545.

42 Sun, D., Gao, Q., Lu, Y., Huang, Z. and Li, T. (2014) 'A novel image denoising algorithm using linear Bayesian MAP estimation based on sparse representation', *Signal Process.*, Vol. 100, pp.132–145.

43 Yue, H., Sun, X., Yang, J. and Wu, F. (2015) 'Image denoising by exploring external and internal correlations", *IEEE Trans. Image Process.*, Vol. 24, No. 6, pp.1967–1982.

Website

Dataset link: http://www.cs.albany.edu/~xypan/research/snr/Kodak.html